Available online at www.sciencedirect.com
SCIENCE DIRECT®
Sensors and Actuators B 93 (2003) 126–134
SENSORS AND ACTUATORS B CHEMICAL
www.elsevier.com/locate/snb

Semiconducting metal oxide sensor array for the selective detection of combustion gases

Alexey A. Tomchenko*, Gregory P. Harmer, Brent T. Marquis, John W. Allen

Sensor Research and Development Corporation, 17 Godfrey drive, Orono, ME 04473, USA

Abstract

A sensor array consisting of discrete thick-film sensors based on various semiconductor metal oxides (SMO) has been designed and fabricated for flue gas analysis purposes. The selection of the sensitive materials for the array has been accomplished as a result of extensive studies of gas-sensitive properties of SMO. The thick-film sensors, prototypes and the array's components, were fabricated on the basis of commercial sensor platforms. A drop-coating technique was used for metal oxide paste deposition followed by in situ drying and annealing of the deposited films in air by platinum heaters integrated into the platforms. We show the results obtained with a variety of thick-film metal oxide species and examine their sensitivities at different fixed operating temperatures (200–400 °C). The feasibility of the electronic system consisted of SnO_2, ZnO, WO_3, CuO, and In_2O_3 sensors to discriminate and recognize various gaseous constituents of a combustion gas is demonstrated. Principal component analysis along with several classification schemes were used to identify nitrogen oxides, ammonia, sulfur dioxide, and other gaseous pollutants.

Keywords: Gas sensors; Metal oxides; Thick films; Sensor array; Principal component analysis

1. Introduction

An electronic sensor system is highly desirable to provide on-line monitoring of the chemical composition of gas emitted from combustion facilities, in order to minimize air pollutions, and maintain the concentrations of dangerous gaseous species within the limits stipulated by regulations. Semiconductor metal oxide (SMO) gas sensors are considered as one of basic technologies for identification and measuring the concentrations of gas in combustion atmosphere [1]. These microelectronic devices offer a wide variety of advantages over traditional analytical instruments such as low cost, short response time, easy manufacturing, and small size. Despite these qualities SMO gas sensors suffer a lack of selectivity. The metal oxides investigated to date are non-selective, i.e. they are sensitive simultaneously to wide range of reducing and oxidizing gases. Some methods to improve SMO selectivity e.g. optimization of operating temperature, bulk/surface doping, use of molecular filters have been successfully employed during the last decades. The implementation of an array of SMO sensors combined with appropriate pattern recognition and classification tools is one of the more promising approaches to compensate for this drawback.

The first report of a sensor array was presented by Persaud and Dodd in the early 1980s [2]. They demonstrated that a cluster of non-selective sensors could be used to discriminate between simple odors through pattern recognition schemes. Since that time, considerable efforts have been made to study sensor arrays for the detection of gases in a large variety of technological fields such as environmental monitoring, food and drink analysis, medical appliances, and industrial control systems [3–5]. It has been shown by many research teams that a sensor matrix based on several technologies or several SMO materials could provide a specific and unique response patterns (chemical fingerprints) for different individual chemical species or mixtures of species. Various pattern recognition techniques have been proposed to analyze sensor array data. Commonly used schemes are principal component analysis (PCA), cluster analysis, artificial neural networks, and specific algorithms based on fuzzy logic [6]. As regards to the requirements imposed on the individual sensors that make up the arrays, they have to be reliable, stable, repeatable and reversible (i.e. being able to recover back to the baseline) in order to avoid retraining of the analytical system.

The authors of this paper have recently studied the gas-sensitive electrical properties of thick- and thin-film

* Corresponding author. Tel.: +1-207-866-0100; fax: +1-207-866-2055.
E-mail address: atomchenko@srdcorp.com (A.A. Tomchenko).

0925-4005/03/$ – see front matter © 2003 Elsevier Science B.V. All rights reserved.
doi:10.1016/S0925-4005(03)00240-5

prototype sensors based on WO_3 [7–9]. An array of two WO_3 Au-doped thin-film sensors was developed for flue gas analysis [9]. It was shown using PCA on the sensor array data that there was good discrimination between the test gases. In particular, the array selectively and repeatedly detected NH_3 and NO_x.

The aim of the present study is to investigate the viability of SMO thick-film gas sensors prepared using cheap commercial sensor platforms and a very simple drop-coating technique accompanied with in situ annealing of the deposited films by the heaters integrated into the platforms. To gain insight to the feasibility of this sensor design modification, a large variety of semiconductor metal oxides traditionally employed in gas-sensors have been tested at different operating temperatures in gas flows containing CH_4, CO, NO, NO_2, NH_3, SO_2, or H_2S. A further objective of this study is to analyze the ability of an array consisting of five selected metal oxide sensors to identify the gases under tests by means of pattern recognition and classification techniques.

2. Experimental

2.1. Fabrication of thick-film sensor arrays

Porous metal oxide thick films approximately 50 μm thick were fabricated using a drop-coating technique and an in situ impact annealing method. The films were deposited onto commercial UST sensor platforms (UST Umweltsensortechnik GmbH) that consisted of 3 mm × 3 mm alumina substrates suspended by platinum leads in TO-8 cases (Fig. 1). The substrates were equipped with integrated platinum heaters and electrodes to the sensitive film. To form the film, a drop of metal oxide paste was applied onto the electrodes. Pastes were prepared by mixing oxide powders with a glass frit and an organic binder. Nanosized powders of SnO_2 and ZnO (Nanophase Technologies Corporation), a sol–gel powder of WO_3 (LASST, University of Maine), and microdispersed powders of CuO and In_2O_3 (Aldrich) were used as base materials. After the thick-film deposition the samples (sensors) were put into a test gas chamber and in situ dried and annealed using the integrated platinum heaters in airflow of 100 cm^3 min^{-1}. The drying was at 150 °C for 15 min, and annealing at 600 °C for 15 min. Prior to the start of each test the sensors were preheated for 60 min at the testing temperature to allow the SMO films to thermally stabilize.

2.2. Gas system and electrical sensing testing

The experimental setup used for electrical testing of the thick-film sensor array is shown in Fig. 2. It consists of the test chamber, a gas delivery system based on the Environics 2000 computerized multi-component gas mixer, a mass flow controller unit, 10-channel multiplexer, 10-channel heater unit, an electrometer for measuring the sensors' resistance, power supplies, and a computer interface for all instrumental equipment. The sensors were operated at 200, 300, or 400 °C by heating the integrated platinum heater with a dc voltage controlled by feedback circuitry described in detail elsewhere [10]. The custom LabVIEW-based software was used for the on-line control of the test setup and measurement of sensors' resistance and temperature. The data recorded from the sensor array was real-time visualized on screen and stored for further processing, analysis and classification. The target gases used were CH_4, CO, NO, NO_2, NH_3, SO_2, and H_2S. Dry air was used as the purge and a carrier gas. Flows containing target gases and the purge were alternately switched to the test chamber with a fixed flow rate of 100 cm^3 min^{-1}.

To determine the sensitivity we use the resistance at the instants immediately before the start and the end of a gas hit (R_i and R_f, respectively). Sensitivity is then defined as $S = R_{max}/R_{min}$, where R_{max}/R_{min} was calculated as R_i/R_f for reducing gases and R_f/R_i for oxidizing gases. The results and analysis described further are in two stages. In the first

Fig. 1. An UST sensor platform suspended by leads to a TO-8 case. The dime (18 mm diameter) shows the relative size of the sensor and case.

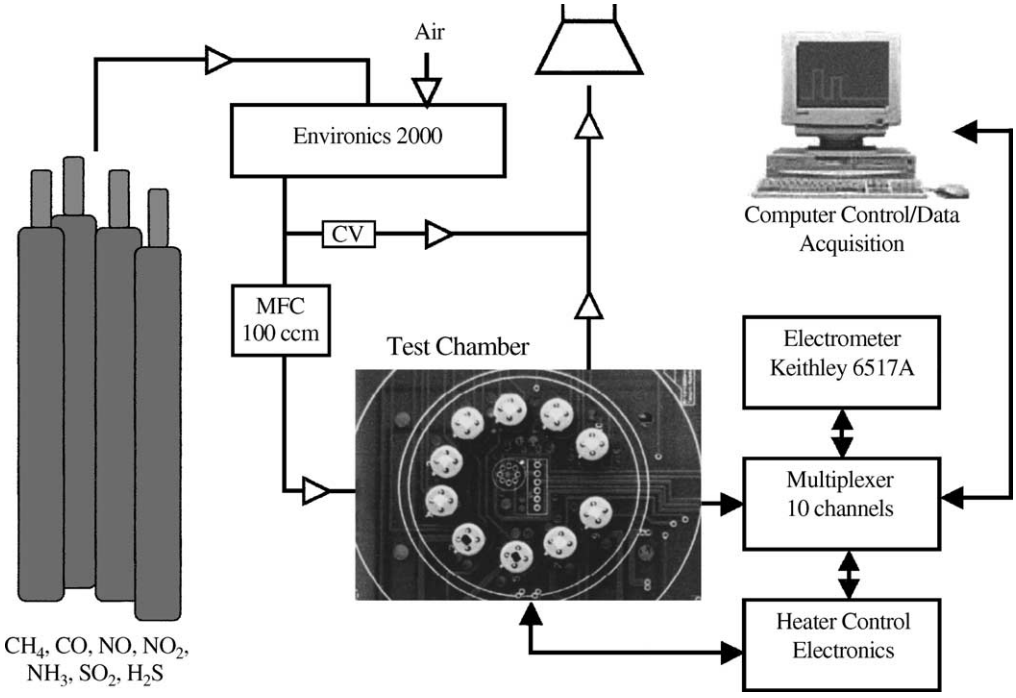

Fig. 2. Block diagram of the experimental testing system.

stage the sensitivities were used to determine the operating temperature that produced the strongest reactions between the films and gas, hence providing the most information rich responses. For the second stage a fresh batch of sensors was used to eliminate any permanent effects caused by possible overheating. The data was then analyzed via principle component analysis and classification methods.

3. Results and discussion

3.1. Gas sensitivity of the individual sensors

Five materials frequently used for sensors, i.e. SnO_2, ZnO, WO_3, In_2O_3 and CuO, were carefully examined relative to critical sensing parameters. These include response magnitude (sensitivity), repeatability, selectivity, and stability. In order to determine an optimal operating temperature of the sensor array, the thick films were studied successively at 200, 300, and 400 °C. The gas-hit sequence used for these tests is shown in Fig. 3. The concentration of the delivered gases were 25 ppm, except for CH_4, which was 30 ppm as to maintain constant flow rates in the system. Each gas exposure was 3 min long, followed by 12 min of air purge. The sequence was repeated six times to assess the short-term repeatability of the sensors' responses. Table 1 summarizes the maximum sensitivities obtained for this stage of the tests. As seen, all types of the sensors under investigation responded to all target gases, i.e. they are non-selective in principle. Four n-type semiconductors (i.e. SnO_2, ZnO, WO_3, and In_2O_3) showed a drastic increase of resistance towards NO and NO_2 exposures and a decrease towards CH_4 and H_2S exposures. On the contrary, CuO based sensors (p-type semiconductor) showed a decrease of resistance for NO and NO_2 and an increase for H_2S. The sensitivity of the CuO sensors was very low even to these active gases. A typical value of CuO sensor response towards 25 ppm of H_2S was approximately 1.2 at 300 and 400 °C. For other gases the magnitudes of the CuO responses were 1.1 (towards NO_2 at 300 °C) or lower. The n-type semiconductors were more active towards the target gases. Along with the general high sensitivity of NO_x and H_2S as mentioned above, some of

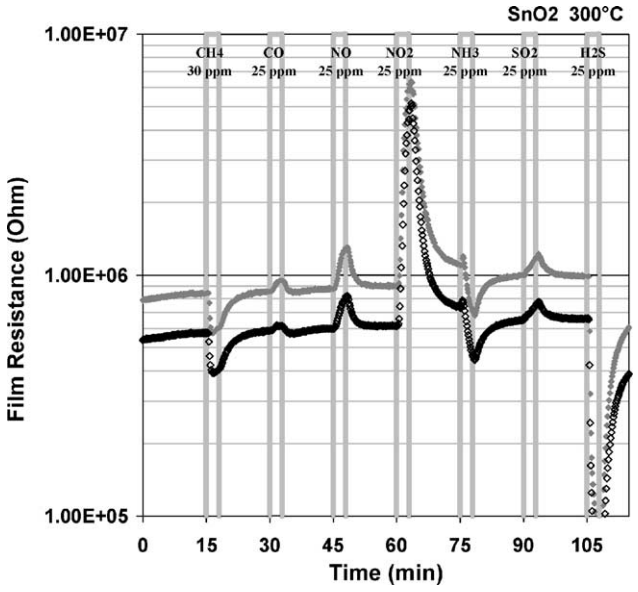

Fig. 3. Gas exposure sequence used at each temperature for determining the optimal operating temperature.

Table 1
Maximum sensitivities observed during the experiments on sensors' operating temperatures

Sensor	Temperature (°C)	Sensitivity (*S*)						
		CH_4	CO	NO	NO_2	NH_3	SO_2	H_2S
SnO_2	200	−1.18[a]	1.40	9.39	4.59	−1.72	1.23	−38.85
	300	−1.30	1.08	2.48	6.13	−1.33	1.13	−14.73
	400	−1.27	−1.09	1.09	1.95	−1.20	−1.03	−6.69
ZnO	200	1.04	3.00	3.53	1.11	−1.10	1.08	−16.90
	300	−1.25	1.56	9.40	11.00	1.20	1.50	−21.67
	400	−1.24	1.01	1.59	5.12	1.08	1.04	−13.16
WO_3	200	−1.10	1.20	8.92	3.73	−1.42	1.3	−34.11
	300	−1.16	1.03	2.56	4.53	−1.04	1.07	−28.18
	400	−1.14	1.01	1.18	3.11	1.11	1.02	−14.02
In_2O_3	200	−1.04	1.56	17.00	6.66	−1.99	1.53	−43.08
	300	−1.04	1.06	1.85	3.42	1.22	1.03	−6.98
	400	−1.02	1.02	1.09	1.40	1.08	−1.01	−2.60
CuO	200	1.01	1.01	−1.03	−1.03	1.02	−1.01	1.16
	300	1.03	1.01	−1.03	−1.09	1.04	1.01	1.18
	400	1.02	1.01	−1.01	−1.04	1.07	1.01	1.24

[a] Minus means that the sensor's resistance decreased during the gas hit. If the resistance increased, the corresponding sensitivity is shown as a positive number.

these materials had a significant response to other gases of interest.

As can be seen from the table, some of the materials demonstrated maximum sensitivity towards particular gases at 200 °C. Nevertheless, the temperature of 300 °C was chosen as the work temperature for the sensors included in the sensor array. The choice was a compromise between the sharp sensitivity drop observed at temperatures above 300 °C, and the sensors' speed of response that only became adequate at 300 °C. As an example, the comparison of the normalized sensors' responses to NO_2 at 200 and 400 °C is given in Fig. 4. The figure shows that the In_2O_3, WO_3, and SnO_2 sensors demonstrated high sensitivity and very slow recovery towards NO_2 at 200 °C (Fig. 4a). On the contrary, the same sensors heated to 400 °C had remarkable recovery after NO_2 hits (about 3 min, see Fig. 4b) but were substantially less sensitive towards this gas. Taking into account that the same tendency was observed for other sensor materials and other gases of interest the temperature of 300 °C has been selected as operating temperature of the investigated sensor array.

3.2. Analysis of response kinetics

For the second stage, a new batch of sensors were prepared and only operated at 300 °C. The sensors were tested

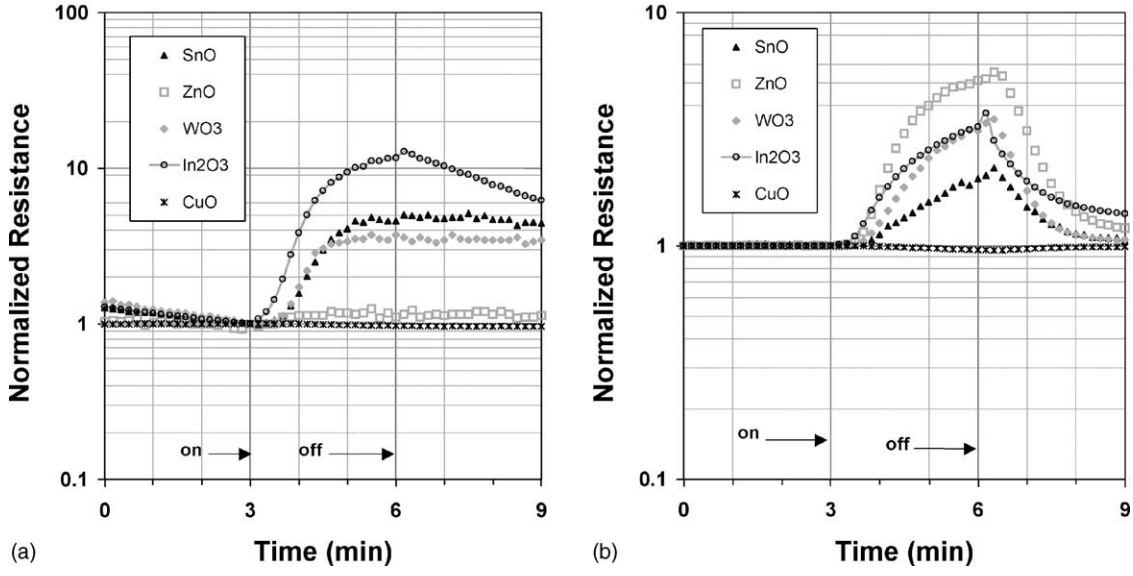

Fig. 4. Normalised response of SMO sensors to NO_2 at: (a) −200 and (b) −400 °C.

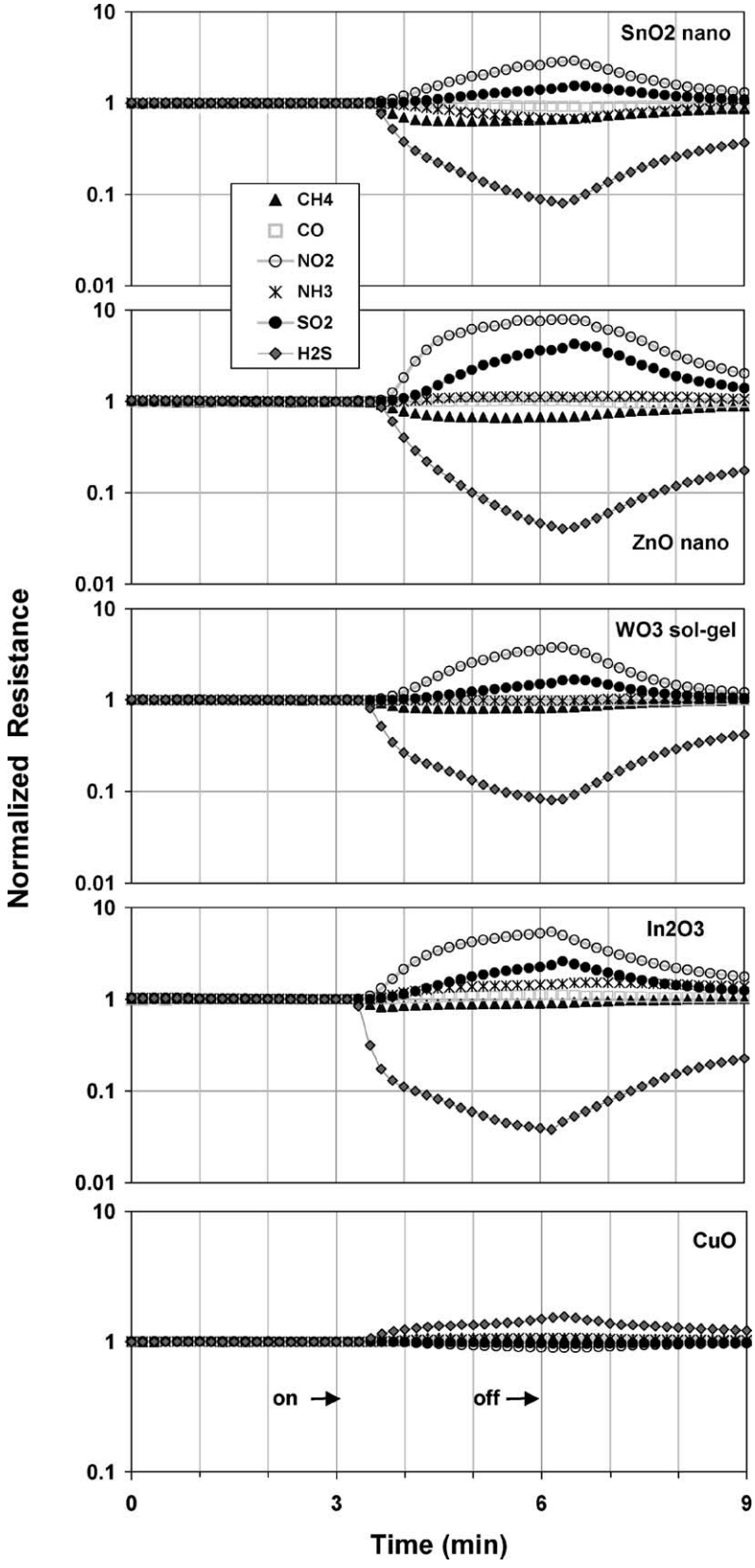

Fig. 5. Baseline normalised responses for all of the sensor–gas combinations. The sensors operated at 300 °C.

over a week, which included five trials, each trial consisting of nine iterations of preheating and the same gas sequence. The sequence of CH_4–CO–NO–NO_2–NH_3–SO_2–H_2S (Fig. 3) was used for three trials, H_2S–NO_2–CO–CH_4–SO_2–NH_3–H_2S for one trial, and different randomized sequences for each of the iterations in the last trial. This was to assess any effects the gas sequence had on the characteristics of sensors' responses.

The typical responses for all of the sensor–gas combinations are shown in Fig. 5. The responses have been normalized to the baseline resistance prior to the gas hit. The marked switching events (i.e. on and off) differ from those observed in the response and are due to the latency of the gas delivery system. This is the time the gas takes to travel from the Environics 2000 to the test chamber (see Fig. 2). This has been taken into account when deriving the features. Even only after observing 3 min of the recovery we can see the responses are quite reversible.

In many papers, the sensors are characterized by their sensitivity [11–14]. However, this captures very little information about the reaction kinetics between the SMO film and gas. It is also strongly influenced by the concentration of the gas. If the concentrations are high and the response saturates (i.e. the reaction reaches equilibrium), or if computational ability is severely limited, it may suffice. To maximize the selectivity we need to extract as much information as possible from the responses during, and after a hit of gas. Therefore, we use a feature that consists of interpolating N points (or gradients) during the hit, and another N points for the first 7.2 min (60% of the recovery period) after the hit.

The characteristics of the response are mainly determined by the type of gas and its concentration, given other operating parameters are constant. The magnitude of the response is primarily controlled by the concentration. Although this also affects the shape of the response, it is minimal compared to influence of the type of gas. Since we wish to identify the gas by their types, and not their concentrations, we have only focused on the shape of the response. The features (in log space) were linearly transformed so the start of the hit was 0 or 1 and the end of the hit was 1 or 0, depending on whether the reaction was oxidizing or reducing. This takes care of baseline normalization and completely eliminates any concentration related sensitivity information. If we wish to determine the concentration, we can reclassify the data using different features with the knowledge of what the analyte is.

Fig. 6 shows the point features for SnO_2 and In_2O_3. For clarity only a couple of the gases have been shown. The data is from three iterations from each trial. The features show good repeatability throughout all the trials. This is important for classification, where we want features that maximize the interclass separation whilst minimizing the intraclass variance.

The main drawback of this strategy is the high dimensional feature space that results. However, employing the commonly used principle component analysis (PCA) to the features greatly reduces this problem.

The PCA algorithm is a popular technique for reducing the dimensionality of data. It is achieved by linearly transforming the data so that correlations between variables are minimized. Even though the PCA itself is lossless, we can remove variables that provide little information about the data to either reduce the dimensionality to an absolute value, or retain a certain percentage of information. To visualize the data we have used PCA to reduce the number of dimensions to three, which allows the data to be conveniently plotted. This representation is useful because it still retains almost all of the characteristics of the full feature space.

Fig. 7 shows the PCA of the data from three trials with different gas sequences (i.e. from one of the trials based on the sequence of CH_4–CO–NO–NO_2–NH_3–SO_2–H_2S, from

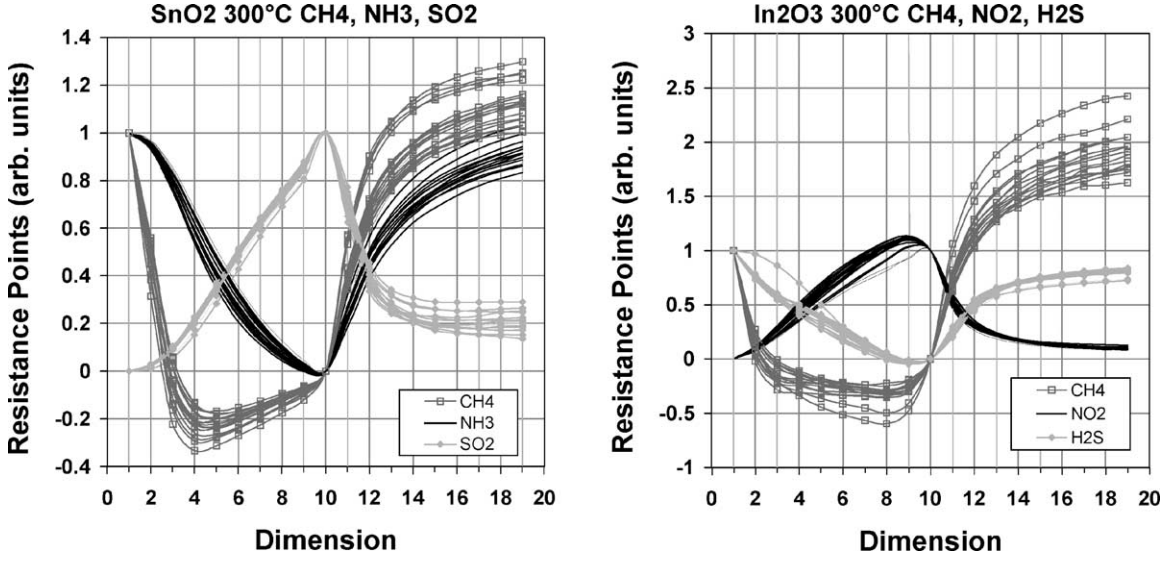

Fig. 6. Extracted features of several gases from SnO_2 and In_2O_3 sensors operating at 300 °C.

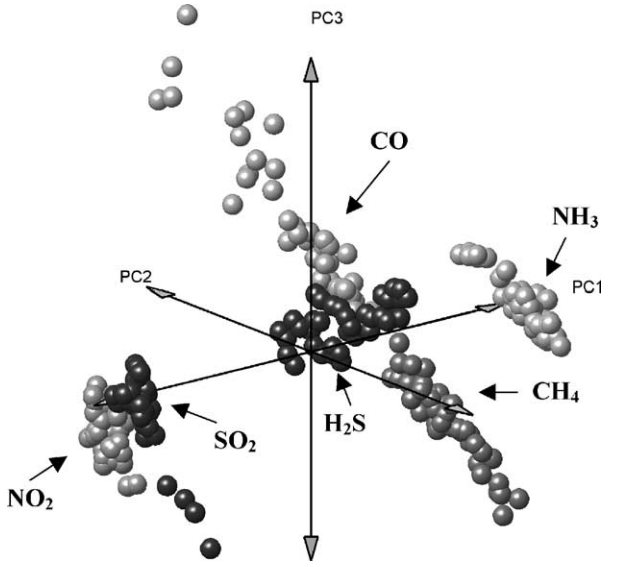

Fig. 7. PCA of three trials. The data is the point features of SnO_2 sensor operating at 300 °C.

the trial based on the sequence of H_2S–NO_2–CO–CH_4–SO_2–NH_3–H_2S, and from the trial consisting of nine iterations with different randomized gas sequences). This PCA shows there is no noticeable discrimination of the data based on the sequence order. It also shows good discrimination between different gases, which means that there is good reproducibility independent of the immediate history of the sensor.

From Fig. 7 we observe that the data clusters into three main groups, (CH_4), (CO, H_2S, NH_3) and (NO_2, SO_2). NO_2 and SO_2 are well separated from the others since they have the only positive responses (see SnO_2 in Fig. 5). The CH_4 is separate from (CO, H_2S, NH_3) as it has a strong reaction, which causes the resistance to drop quickly. The remaining group (CO, H_2S, NH_3) are the slower reacting negative shaped responses. When we look at Fig. 5, the magnitudes of H_2S and CO (which are both in the same PCA cluster) are vastly different. The reason they cluster together is they have a similar shape once we ignore the magnitude differences, thus the extracted point features are similar. If we wish to additionally utilize magnitude information, we can use the gradients features. This will easily separate H_2S from CO and NH_3.

The type of behavior shown in Fig. 7 lends itself to hierarchical classification. Instead of classifying all the gases at once, we first classify them as belonging to one of the aforementioned groups; we then reclassify using only the features of the chosen group to train the classifier. When this is done with the data present in Fig. 7 each gas is easily separated. However, this technique was not implemented automatically for this data.

Though PCA is a powerful tool for discriminating between responses, it does not make a decision as to the identity of the gas—it is merely a clustering technique. To do this, several classification methods have been investigated [15,16]. If computational power is not a limiting factor the full feature space can be used as the input feature, otherwise the PCA transformed data can be used. The classification schemes investigated are briefly described further.

- *Distance measures*: One of the simplest schemes is to assign the unknown feature to the class of the training feature that most closely matches the test feature. In feature space this translates to the training point that is geometrically closest to the test point. This is referred to as template matching or the nearest neighbor. More generally we can use the k nearest neighbors (k-NN) and assign the class with the majority of the k neighbors. Furthermore, we can utilize all the training points by using Shepard's method, which weights them according to their distance from the test point. The class with the highest total weight is the one that is selected. For both of these methods there are a number of distance and weighting functions.
- *Bayesian methods*: If we know in advance the probability density function (PDF) of the classes, we can use Bayes optimal decision rule to find the optimal boundary. The boundary is formed where the PDFs of adjacent classes in feature space are equal. In practice it is rare that we know the distribution in advance. However, if we assume a particular distribution, usually Gaussian, we can estimate the parameters from the training data and hence determine the boundaries. This is referred to as Bayes plug-in rule.
- *Support vector classifier (SVC)*: The SVC is a non-parameterized method (in terms of PDF) for defining optimal separating hyperplane between two classes. By using a nonlinear kernel function we effectively warp the hyperplane to shape it to the data. A cost function is employed to control the trade-off between generalization and over-fitting. As the SVC is only a two-class classifier, multiclass problems are divided into several two-class problems. A boundary is found for each class against the others, we then use the class with the highest confidence. We are currently investigating polynomial (degree 2 and 3), and radial basis function kernels.
- *Neural networks (NN)*: These are very commonly used to analyze sensor array data [12,13,17], possibly due to their high level of abstraction. The architecture that has proved most fruitful is the feedforward backpropagation using a Bayesian regularization process for training. This minimizes the sum of the mean square error (MSE) and mean square weights (MSW). The inclusion of the MSW in the objective function reduces the networks ability to learn, thus avoids over-fitting when there are too many neurons in the hidden layer. This eliminates much of the trial and error in finding the optimal number of neurons to include in the hidden layer.

When using the classifiers, the hold-out method was employed. We set 75% of the available data (randomly selected) for training and the remaining 25% as the unknown data to be classified. This means that the data to be classified has never been seen by the classifier. The results of the

Table 2
Percentage correctly classified using the hold-out method (75% train, 25% test)

Sensor	Points	Slopes	PCA points	PCA slopes
CuO	91.53	91.01	86.51	86.24
In_2O_3	94.44	95.24	85.45	93.65
SnO_2	99.74	99.21	99.74	98.68
WO_3	96.53	96.53	96.53	93.06
ZnO	94.97	98.94	90.48	94.71
In_2O_3/SnO_2	–	–	98.68	98.41
CuO/ZnO	–	–	94.44	96.56
$CuO/ZnO/In_2O_3$	–	–	94.97	98.41
$WO_3/ZnO/In_2O_3$	–	–	94.44	96.83

individual classifiers are then combined using the median function to make a final decision [18,19]. Almost all of the data from the five trials was used, which gave a total of 378 features per each sensor type. Though a couple of bad iterations were excluded, there still remained some bad features that were clearly different from the others of the same class. The point features were directly fed into the classifiers, whereas the gradient and PCA transformed features were standardized to a zero mean and unity variance for each dimension. The standardization was not necessary for the point features due to the transforms used to generate them.

Table 2 shows the results of the classifiers using individual and combined features averaged from three runs. For the hit and recovery times used, some of the individual sensors were selective enough to identify the gasses with a high degree of accuracy. It is likely that many of the errors were due to bad features. For the individual sensors, SnO_2 clearly outperformed the others with almost 100% classification rate. Generally, PCA transformed features did not classify as well as the full features. This implies that the small amount of information that was discarded is important [20]. Possibly retaining more PCs, 5–6 for example, would give more comparable results to the full features.

The bottom four rows of Table 2 show the classification results when the principle components of the individual sensors are combined. From the In_2O_3/SnO_2 results, we see that the poor selectivity of In_2O_3 actually degrades the performance of the (individual) SnO_2 sensor. However, when combining the features of sensors that both have poor selectivity the performance can be improved. This is particularly noticeable with the $CuO/ZnO/In_2O_3$ combination where we have a 4–10% improvement in classification compared to the individual sensors. The results could be further improved by combining different types of features from different sensors.

4. Conclusions

A sensor array of five thick-film SMO sensors has been fabricated using cheap commercial sensor platforms and a drop-coating technique accompanied with in situ annealing of the deposited films by the heaters incorporated into the platforms. Five different SMO materials, namely, SnO_2, ZnO, WO_3, In_2O_3 and CuO, were carefully examined relative to sensitivity towards CH_4, CO, NO, NO_2, NH_3, SO_2, and H_2S. The sensors included in the array demonstrated their functional performance as sensing devices. They were reliable, stable, and reversible relative to the gases of interest. The optimal operating temperature of the sensor array has been determined as a result of extensive SMO tests accomplished at different operating temperatures.

The feasibility of the sensor array to discriminate and recognize various gaseous constituents of a combustion gas has been demonstrated in the paper. Principal component analysis along with several classification schemes were used to identify nitrogen oxides, ammonia, sulfur dioxide, and other gaseous pollutants. To further improve classification results, a hierarchical technique could be employed. The clustering shown in the PCA plots suggest that this method would work well. The disadvantage is that we need to know the hierarchical groups beforehand, unless some type of unsupervised clustering method can be used.

In the future, we plan to expand the testing to a continuous range of concentrations. In this stage the strength of using a sensor array should become clear. To determine the concentration, an extra classification layer will be added that reclassifies the gas in terms of its concentration, once its identity is know. The features used to train these classifiers will be different since the magnitude information now becomes important.

Acknowledgements

This work was supported by Sensor Research and Development Corporation under contract # N00014-01-C-0132 from the Office of Naval Research, USA. The authors thank the Laboratory for Surface Science and Technology (LASST) of the University of Maine for the preparation of the WO_3 sol–gel powder.

References

[1] A.B. Tomkings, Advanced sensors for environmental monitoring in fossil-fired power plant, Sens. Rev. 17 (1997) 311–315.
[2] K. Persaud, G.H. Dodd, Analysis of discrimination mechanisms of the mammalian olfactory system using a model nose, Nature 299 (1982) 352–355.
[3] J.W. Gardner, P.N. Bartlett, A brief history of electronic noses, Sens. Actuators, B Chem. 18–19 (1994) 211–220.
[4] W. Gopel, Chemical imaging: I. Concepts and visions for electronic and bioelectronic noses, Sens. Actuators, B Chem. 52 (1998) 125–142.
[5] J.W. Gardner, P. N. Bartlett, Electronic Noses, Oxford University Press, Oxford, 1999.
[6] A. Ahluwalia, D. De Rossi, 2000. Artificial noses and tongues, in: K.H.J. Buschow, R.W. Cahn, M.C. Flemings, B. Ilschner, E.J.

Kramer, S. Mahajan (Eds.), Encyclopedia of Materials: Science and Technology, Elsevier, Oxford.
[7] A.A. Tomchenko, V.V. Khatko, I.L. Emelianov, WO_3 thick films gas sensors, Sens. Actuators, B Chem. 46 (1998) 8–14.
[8] A.A. Tomchenko, Structure and gas-sensitive properties of $–Bi_2O_3$ mixed thick films, Sens. Actuators, B Chem. 68 (2000) 48–52.
[9] B.T. Marquis, J.F. Vetelino, A semiconducting metal oxide sensor array for the detection of NO_x and NH_3, Sens. Actuators, B Chem. 77 (2001) 100–110.
[10] J.W. Allen, B.T. Marquis, D.J. Smith R., Investigating the long-term heating and analyte exposure effects on tin oxide thick-film sensors, IEEE Sensors 2002, in: Proceedings of the First IEEE International Conference on Sensors, vol. 2, Orlando, FL, USA, 11–14 June 2002, pp. 1260–1265.
[11] D.S. Lee, H.Y. Jung, J.W. Lim, M. Lee, S.W. Ban, J.S. Huh, D.D. Lee, Explosive gas recognition system using thick film sensor array and neural network, Sens. Actuators, B 71 (2000) 90–98.
[12] H.K. Hong, C.H. Kwon, S.R. Kim, D.H. Yun, K. Lee, Y.K. Sung, Portable electronic nose system with gas sensor array and artificial neural network, Sens. Actuators, B 66 (2000) 49–52.
[13] M. Penza, G. Cassano, F. Tortorella, G. Zaccaria, Classification of food, beverages and perfumes by WO_3 thin-film sensors and pattern recognition techniques, Sens. Actuators, B 73 (2000) 76–87.
[14] M. Penza, G. Cassano, F. Tortorella, Gas recognition by activated WO_3 thin-film sensors array, Sens. Actuators, B 81 (2001) 115–121.
[15] A.K. Jain, R.P.W. Duin, J. Mao, Statistical pattern recognition: a review, IEEE Trans. Pattern Anal. Machine Intel. 22 (2000) 4–37.
[16] J. Lampian, J. Laaksonen, E. Oja, Neural network systems, techniques and applications in pattern recognition, Research Reports B1, EE Department, Helsinki University of Technology, 1997.
[17] J.C. Chen, C.J. Liu, Y.H. Ju, Determination of the composition of NO_2 and NO mixture by thin film sensor and back-propagation network, Sens. Actuators, B 62 (2000) 143–147.
[18] L.I. Kuncheva, On combining multiple classifiers, in: Proceedings of the 7th International Conference on Information Procedure And Management of Uncertainty, Paris, France, 1998.
[19] J. Kittler, M. Hatef, R.P.W. Duin, J. Matas, On combining classifiers, IEEE Trans. Pattern Anal. Machine Intel. 20 (1998) 226–239.
[20] M. Pardo, G. Sberveglieri, A study in the application of multilayer perceptions to the analysis of chemical sensors systems data, IEEE Sensors 2002, in: Proceedings of the First IEEE International Conference on Sensors, vol. 2, Orlando, FL, USA, 11–14 June 2002, pp. 1304–1307.

Biographies

Alexey A. Tomchenko was born in 1958 in Minsk, Belarus. He received the MSc degree in electronic engineering in 1984 from Minsk Radio Engineering Institute and the PhD degree in electronic engineering in 1999 from the Institute of Electronics of the National Academy of Sciences of Belarus. In 1981–2000 he worked at the Physical Technical Institute of the Academy of Sciences of Belarus, Minsk, first as a Test Engineer and then as a Researcher of the staff. He has been with Sensor Research and Development Corporation since 2000 and is currently a Senior Research Scientist. His research interests are chemistry, physics and technology of oxide films, chemical gas sensors and sensor arrays.

Gregory P. Harmer received the BSc (applied maths and computer science) degree in 1996, the BE (electrical & electronic engineering) degree in 1997 and the PhD in 2001, all from the University of Adelaide. He was an invited speaker at UPoN'99, Adelaide, Australia. He currently works at Sensor Research & Development Corporation and is studying sensor noise and signal processing techniques for sensor arrays.

Brent T. Marquis received his BS and MS degrees in electrical engineering from the University of Maine in 1996 and 2000, respectively. He joined SRD in 1995 as a research engineer and is now their Director of Research Engineering. He has over 10 years of SMO and SAW sensor research and development experience and has published several papers related to SMO sensors, platforms, and operational characterizations. Mr. Marquis has expertise in SMO platform development, sensor testing systems design, thin- and thick-film development, and data processing in support of on-board computational power for miniaturized sensors. Mr. Marquis has special technical expertise in thin-film deposition and metal oxide film design and engineering for selective detection of chemical warfare agents, combustion gases, and halogenated hydrocarbon species, as well as extensive experience in the development of adaptable sensor platforms for a variety of harsh industrial environments. He has been SRD's principal investigator on several sensor programs for the Department of Defence, the Department of Energy, and the National Science Foundation.

John W. Allen was born in Bangor, ME, on 1 October 1973. He received BS and MS degrees in electrical engineering from the University of Maine in 1996 and 1999, respectively. He has worked in industry as an electrical engineer specializing in sensor research and analog circuit design for over 6 years. He is currently a senior research engineer at Sensor Research and Development Corporation in Orono, ME.